Korean J. Chem. Eng., 39(11), 2896-2906 (2022)
DOI: 10.1007/s11814-022-1225-x

pISSN: 0256-1115
eISSN: 1975-7220

REVIEW PAPER

Fluid dynamics, velocity profile and average cycle time in different configurations of the modified mechanically stirred spouted bed

João Pedro Alves de Azevedo Barros†, Fábio Bentes Freire, and José Teixeira Freire

Federal University of São Carlos, Department of Chemical Engineering, Rod. Washington Luiz - Km 235, P. O. Box 676, 13565-905, São Carlos, SP, Brazil

(*Received 27 January 2022 • Revised 14 June 2022 • Accepted 4 July 2022*)

Abstract−We analyzed modified spouted bed configurations incorporating three different types of mechanical stirrer, in comparison to a conventional spouted bed. Straight-blade, inclined-blade, and helical screw agitators were used with different types of inert particles. The behavior of the fluid dynamic curves was qualitatively similar for the systems with agitators and the conventional design, except for the screw-type agitator. For the straight-blade and inclined-blade agitators, increase of the rotation speed had a positive effect on the fluid dynamic parameters, reducing the air flow and the pressure drop in the bed. The effects of rotation speed and blade inclination on the fluid dynamics were minimized at 240 rpm, although the mass of particles could influence these parameters. The inclined-blade stirrer performed the best, reducing airflow between 40 and 66% compared to the conventional spouted bed. For the screw-type stirrer, the reduction was around 27% in some of the experiments. The rotation speed of the stirrer and the air flow to agitate the bed affect the average cycle time of the process, with a stronger effect on the rotation speed. Overall, the use of the stirrers in the bed provided significant improvement, with reduction of both the air flow, the pressure drop and average cycle time, as well as greater stability of the bed.

Keywords: Mechanical Stirring Spouted Bed, Cycle Time, Velocity, Fluid Dynamic

INTRODUCTION

The spouted bed is an excellent option for industrial applications requiring a high degree of fluid-solid contact, due to the high particle circulation rate, which provides a homogeneous bed of particles and high rates of heat and mass transfer [1-3]. Spouted beds are used in coating processes [4,5], granulation [6], solids feeding [7], and in chemical, electrochemical, and pyrolysis reactors [8-12], in addition to being used for drying solid materials, pastes, and solutions [2,13-16].

Although intense movement of the particles is an advantage in most operations performed with this equipment, in some situations it may be a disadvantage. For example, Brito et al. [15] reported the negative effect of intense particle movement on the germination capacity of grains, due to the many collisions among the particles and the walls of the equipment. In studies of the drying of pastes and solutions, operational problems were observed, due to agglomeration and accumulation of the product in the bed [14,17,18]. In such cases, lack of control of the movement of the particles can prejudice the process, consequently decreasing the quality of the final product.

In a spouted bed, circulation of the particles occurs due to the high air flow required for motion of the particles in the bed and maintenance of stability in the system, with a large part of this flow not being used for the drying itself, but instead to move the particles in the bed [19,20]. Furthermore, the higher air flow increases energy consumption, especially in drying processes, which can hinder use of these systems in industrial applications. Therefore, spouted beds have been modified with the aim of minimizing the negative effects caused by high air flow, including use of agitated fluidized beds [21-24], conical spouted beds [25,26], spouted beds with internal devices (draft tubes and fountain confiners) [27-30], and spouted beds with mechanical stirrers [19,31-35].

The spouted bed equipped with a mechanical stirrer is a promising system that offers advantages over other configurations. Its first version was developed in the mid-1970s by a group of researchers at the Hungary Research Institute, employing a helical screw type stirrer [33,34,36,37]. The equipment was defined as a mechanical spouted bed (MSB), with the main difference, compared to a conventional system, being the installation of a helical screw along the vertical axis of the spouted bed, with the air feed supplied laterally, at a tangent to the bed. Reyes and Vidal [31] modified the MSB, changing the type of stirrer (conical) and the air feed (ascending, as in the conical spouted bed - CSB). This new version was denoted a mechanically stirred spouted bed (MSSB). Sousa et al. [38] also described a modified version of the MSB with ascending feed, but maintaining the screw-type stirrer, which was denoted a modified mechanical spouted bed (MMSB). Despite these modifications, operational problems in the bed were observed, such as particle agglomeration and dead zones, because the diameter of the bed cylinder was much larger than the diameter of the stirrer. To resolve these problems, Barros et al. [32] used a new type of stirrer (paddle shape) to improve movement of the particles in the bed, which gave better results compared to conventional equipment. This system was

†To whom correspondence should be addressed.
E-mail: joaopedroaab@gmail.com

denoted a modified mechanical stirring spouted bed (MMSSB).

The various modifications of the spouted bed with mechanical agitation have their own peculiarities, although in all cases the use of mechanical agitation in the bed has been shown to provide advantages, compared to conventional equipment. The main benefits include reduction of internal pressure peaks [32,34], lower energy consumption, due to the lower air flow required to operate the equipment [37,39], improved bed stability, and increased maximum drying capacity, as well as avoidance of particle agglomeration and product accumulation in the equipment [23,31]. An important feature is the ability to control the stirrer rotation speed, enabling finer adjustment of the particle circulation rate [35], because the particles are mainly moved by the action of the stirrer, rather than by the air flow as in the case of conventional equipment. For optimization of operations using mechanically agitated beds, it is essential to consider the geometry of the stirrer and the way that it affects the process parameters.

Despite the advances described above, there have been few detailed studies of the influence of different stirrers on the behavior of the particles inside spouted beds equipped with mechanical stirrers. Therefore, the aim of the present work was to perform a fluid dynamic characterization of the MMSSB with different configurations of stirrers, analyzing the effect of rotation speed on the fluid dynamic parameters. To compare the different stirrer configurations, the air velocity profile and the average cycle time of the particles in the bed were analyzed. For the purpose of comparison of the MMSSB with other configurations, the same experiments were also performed with the CSB. Different groups of particles were used, with analysis of particle diameter, density, sphericity, geometry, and bed mass. Inert particles are commonly used in drying operations [2,14,38,40], providing representative parameters applicable to various particulate systems. The results provide a better understanding of the effects of different stirrers in beds of particles, assisting in identification of the stirrer that is most suitable, considering the operational parameters of the equipment.

MATERIALS AND METHODS

The experiments employed a conical-cylindrical spouted bed constructed of stainless steel with an external angle of 60°. The stirrer was inserted in this conventional equipment, converting it to an MMSSB. The specifications for the stirrer with straight blades are shown in Fig. 1(a). The same configuration was used for the stirrer with inclined blades, only changing the blade angle to 45°. The helical screw stirrer (Fig. 1(b)) was the same model used in the work of Sousa et al. [38]. A perforated air distributor was placed on the conical base of the bed to provide a more homogeneous distribution of the air flow and support the stirrer, which ensured the stability of the system (avoiding vibrations), as demonstrated in preliminary tests. This distributor was only used for the experiments employing the MMSSB. However, due to the experimental methodology, which was originally developed by Mathur and Epstein (1974) for the conventional spouted bed, there was little influence from the air distributor. Additional details of the experimental unit, data acquisition, storage procedure and stirrer design can be found in previous reports [14,32].

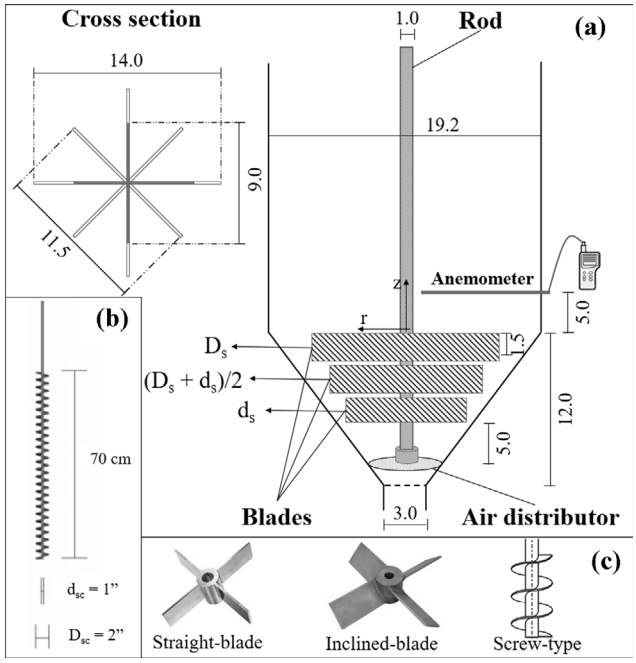

Fig. 1. Dimensions (in cm) of the straight-blade stirrer (a) and the helical screw stirrer (b). Representative illustration of the three agitators used (c). Fig. 1(b) adapted from Sousa et al. [38].

The solids used in this study were particles of glass, alumina, and polyethylene, defined as group D, according to the Geldart classification [41]. These particles have been used in other studies and are considered suitable for experiments that involve particle movement [19,32,35] and for use as a support medium for the drying of pastes and solutions [14,38]. Details of the particles and the assays used are provided in Table 1.

Characterization of the fluid dynamics of the conventional spouted bed follows the procedure described by Mathur and Epstein [42], based on a graph of the pressure drop in the bed according to increasing or decreasing air flow. This graph can be used to obtain information including the minimum spouting air flow (Q_{ms}), the maximum pressure drop (ΔP_{max}), and the stable pressure drop (ΔP_s). For the modified mechanically stirred spouted bed, a similar procedure was used to obtain fluid dynamic parameters including the minimum air flow for stirring of the bed (Q_{sb}) and the operational pressure drop for stirring of the bed (ΔP_{sb}). Further details of this procedure can be found in a previous study [32].

For equipment with mechanical agitation, assays were performed using rotation speeds of 0, 12, 21, 60, 90, 120, 198, 240, 291, and 330 rpm. In addition to this parameter, the effects of the types of stirrer and particles were investigated. All the assays were performed in triplicate.

The relative reduction parameter (RR) was used to estimate the increase or decrease of the air flow for each configuration, compared to the conventional equipment, with Eq. (1).

$$RR\,(\%) = \frac{(Q_{ms} - Q_{sb})}{Q_{ms}} 100 \quad (1)$$

A hot wire anemometer (AKSD-AK833) was inserted trans-

Table 1. Particle properties and experimental conditions used for the mechanically stirred and conventional spouted beds

Assay	Material	ρ_p (kg m^{-3})	d_p (m)	ϕ	ε	Bed mass (kg)
E1	Glass	2,500	0.0022	1.0	0.424±0.001	2
E2						3
E3						4
E4			0.0044	1.0	0.434±0.003	2
E5						3
E6						4
E7	Alumina	1,501	0.0037	1.0	0.501±0.006	2
E8						3
E9						4
E10	Polyethylene	930	0.0037	0.93	0.435±0.005	2
E11						3
E12						4
E13	Polyethylene	930	0.0038	0.37	0.514±0.002	2
E14						3
E15						4

versely 0.05 m above the base of the cylindrical column, for measurement of the air velocity as a function of the radius, in position z (Fig. 1). The measurements were made (in triplicate) during 10 s in several radial and angular positions, at a sampling rate of 1.25 Hz. Throughout the measurement period, the air temperature remained at 29.7±0.8 °C. The average cycle time was analyzed with alumina particles (E8), two of them of different colors (red and blue) placed on the surface of the bed. By filming the free surface of the bed, the time taken for the particle to reemerge at the top of the bed was measured, thus determining the average cycle time of the particles. A similar procedure was adopted by Szentmarjay et al. [35]. The average number of measurements was approximately 110±30 points for each experiment performed. Thus, after filming the bed surface, the images were digitally processed with reduced playback speed to measure the return time of each particle to the surface. The effect of average cycle time in the process was analyzed for each mechanical stirrer configuration. The parameters analyzed were rotation speed and air flow to stir bed (Q_{sb}). To analyze the effect of process variables, it used different rotational speeds from 90, 120, and 240 rpm and air flow to stir the bed 1.00 Q_{sb}, 1.25 Q_{sb} and 1.50 Q_{sb}.

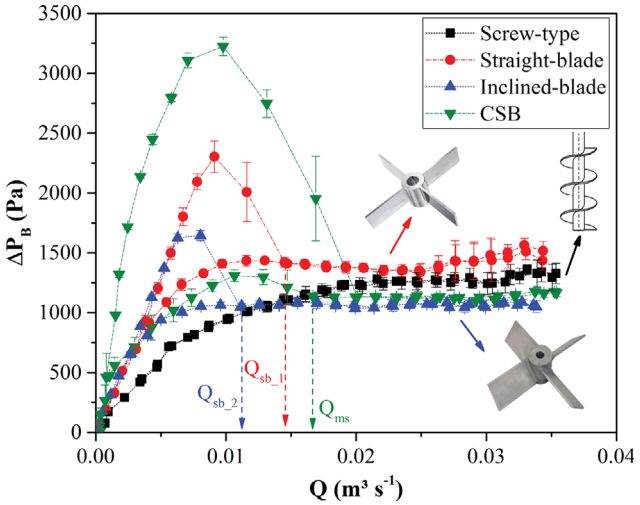

Fig. 2. Pressure drop, as a function of air flow rate, for the conventional spouted bed and the systems with different mechanical stirrer configurations. Conditions: Glass particles (d_p=2.2 mm and load of 3 kg) and rotation speed of 60 rpm.

RESULTS AND DISCUSSION

1. Characteristic Fluid Dynamics of Spouted Bed with and without Mechanical Stirring

Fig. 2 shows the characteristic fluid dynamic curves (pressure drop as a function of air flow rate) for the CSB and for the MMSSB with different stirrers. A rotation speed of 60 rpm was used for the configurations with stirrers. The behavior for the inclined-blade and straight-blade stirrers was qualitatively similar to that of the conventional equipment. The inclined-blade stirrer provided greater reduction of the maximum and stable regime (operational) pressure drops, compared to the straight-blade stirrer. In addition, the operational pressure drop for the inclined-blade stirrer was lower than obtained for the conventional spouted bed, even at a rotation speed of 60 rpm. This was due to the inclination of the blades, which favored upward movement of the particles, consequently improving their motion in the bed. These results were in agreement with previous work showing that the use of inclined-blade stirrers can provide better improvement of the pressure drop, compared to other configurations [22].

The method used to determine the air flow required to agitate the bed (Q_{sb}) was as described by Barros et al [32]. The air flow for the inclined-blade stirrer (Q_{sb_2}) was around 32% lower than for the straight-blade stirrer (Q_{sb_1}) and 38% lower than for the conventional equipment (Q_{ms}), indicating that better performance could be achieved using blades with some degree of inclination. It was

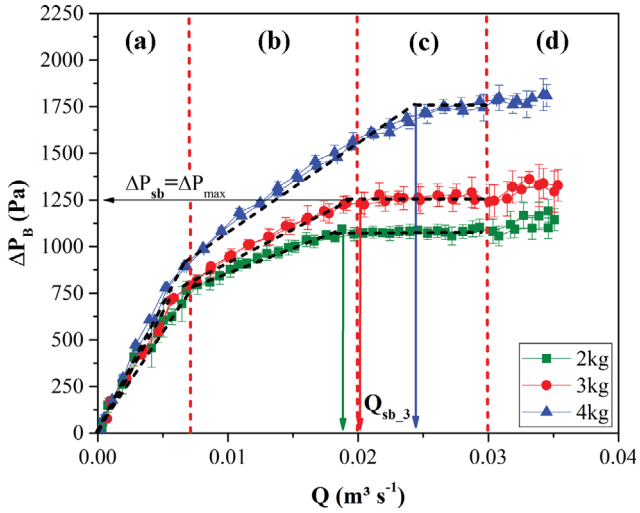

Fig. 3. Pressure drop according to air flow for the spouted bed with a helical screw mechanical stirrer, operated at 120 rpm with 2.2 mm glass particles. Regions (a), (b), (c), and (d) are delimited based on the curve for load of 3 kg of particles.

not possible to use the same method to determine the air flow for the screw-type stirrer, because the fluid dynamic behavior (Fig. 2) differed significantly from that of the other configurations. Hence, a different procedure was used to estimate the air flow required for stirring of the bed using the helical screw (Q_{sb_3}), as shown in Fig. 3.

The characteristic fluid dynamic curves for different particle masses had four regions with different slopes, shown as regions A, B, C, and D in Fig. 3. The intersections between the regions were determined for the experiment with 3 kg of particles, but the same procedure could have been done for the other operating conditions with the screw-type stirrer. The steepest slopes in region A indicated compaction of the particles in the bed, with rapid linear increase of the pressure drop as the air flow increased. Nonetheless, the slopes were lower than obtained using the other stirrers and the conventional spouted bed (Fig. 2), reflecting the influence of the type of stirrer employed. In region A, the effect of the particle mass was not significant. However, the effect of mass was significant in region B, with greater mass leading to a higher pressure drop with increase of the flow. In region C, the pressure drops remained almost constant with variation of the air flow.

It can be seen (Fig. 3) that the slope of the line in region B is lower than in region A. This could be explained by the effect of bed expansion, for which there was a limit indicated by the maximum value of the pressure drop observed between regions B and C. At the interface between these two regions, it was possible to estimate the air flow required to stir the bed (Q_{sb_3}) and the operational pressure drop, which was equal to the maximum pressure drop, as shown in Fig. 3. Reyes and Vidal [31] for an MSSB used a similar procedure with conical stirrer, where a pseudo-fluidized condition of the bed was observed from a fluid dynamic curve analogous to those shown in Fig. 3.

In region C, increase of the air flow did not alter the pressure drop, because the average porosity of the bed had reached a maximum value that remained constant with increase of the air flow, under stable spouting operational conditions. After region C, the air velocity approached the terminal velocity of the particles, leading to their entrainment. Hence, region D was delimited by instability caused by the high air flow, in some cases presenting the bubbling bed phenomenon.

The data shown in Fig. 3 were obtained for a fixed rotation speed of 120 rpm, since the effect of this parameter had been previously evaluated in initial tests showing that there were no significant differences between the fluid dynamic curves for different rotation speeds, in agreement with the literature [38]. Hence, the air velocity and pressure drop values remained constant as the rotation speed increased. This could be analyzed according to the fluid dynamic

Table 2. Fluid dynamic parameters for the different stirrers in assay E2 performed using 3 kg of glass particles (d_p=2.2 mm)

Ω (rpm)	Stirrers	u_{sb} (m s^{-1})	ΔP_{sb} (Pa)	ΔP_{max} (Pa)
Without stirre	CSB*	21.7±0.5	1,140.0±10.0	3,200.0±60.0
60	Straight-blade	$20.7\pm0.4^{bB**}$	$1,400.0\pm40.0^{aB}$	$2,300\pm200^{aB}$
	Inclined-blade	15.7 ± 0.1^{cA}	$1,040.0\pm10.0^{abA}$	$1,680.0\pm20.0^{bB}$
	Screw-type	27.0 ± 2.0^{aA}	$1,300.0\pm200.0^{bA}$	$1,300.0\pm200.0^{bA}$
90	Straight-blade	19.0 ± 1.0^{bBC}	$1,400.0\pm10.0^{aB}$	$2,150.0\pm70.0^{aB}$
	Inclined-blade	15.0 ± 1.0^{cA}	$1,150.0\pm3.0^{cC}$	$1,700.0\pm100.0^{bB}$
	Screw-type	26.0 ± 1.0^{aA}	$1,260.0\pm20.0^{bA}$	$1,260.0\pm20.0^{cA}$
120	Straight-blade	18.3 ± 0.1^{bC}	$1,430.0\pm40.0^{aB}$	$2,100.0\pm50.0^{aB}$
	Inclined-blade	14.6 ± 0.8^{cA}	$1,110.0\pm40.0^{cC}$	$1,700.0\pm60.0^{bB}$
	Screw-type	26.0 ± 1.0^{cA}	$1,250.0\pm70.0^{bA}$	$1,250.0\pm70.0^{cA}$
240	Straight-blade	14.8 ± 0.2^{bA}	$1,090.0\pm60.0^{bA}$	$1,400.0\pm200.0^{aA}$
	Inclined-blade	13.0 ± 1.0^{bA}	900.0 ± 7.0^{cB}	$1,260.0\pm40.0^{aA}$
	Screw-type	25.2 ± 0.4^{aA}	$1,220\pm60.0^{aA}$	$1,220\pm60.0^{aA}$

*For the conventional spouted bed, the minimum spouting velocity (u_{ms}) was used.
**ANOVA and Tukey's test for the three stirrers operated at a fixed rotation speed (lowercase letters) and at different rotation speeds for the same type of stirrer (uppercase letters).

parameters for the same particle group and load (Table 2).

The same pressure drop was measured for both the increase and decrease of the airflow rate, as can be seen in Fig. 3 by the superposition of the experimental data. This is due to the geometry of the helical screw type mechanical stirrer with a smaller diameter than other stirrers, which allows the screw-type stirrer to be placed between the air distributor and the bed surface, modifying the movement of the particles. In this way, there is no fixed bed between the air distributor and the beginning of the stirring system, contrary to what happens with other stirrers. Therefore, the screw-type mechanical stirrer reduced the maximum pressure drop even at low rotation speeds, unlike other stirrers. This was because the screw-type stirrer did not generate a thin fixed bed in the space between the air distributor and the beginning of the stirrer (Table 2). This effect was investigated previously by Barros et al. [32] for the straight-blade stirrer [32].

For the three stirrers operated at the same rotation speed (lowercase letters in the Tukey test), the best u_{sb} results were obtained using the inclined-blade stirrer, while the screw-type stirrer was the least favorable. The subsequent replacement of the helical screw with the inclined-blade stirrer decreased the u_{sb} of approximately 42, 42, 44 and 48% to 60, 90, 120 and 240 rpm, respectively. The maximum pressure drop was highest for the straight-blade stirrer under all conditions, except for a rotation speed of 240 rpm, at which this parameter showed no difference among the three stirrers.

Experimental data from u_{ms} and u_{sb} are essential not only for the design, modeling and simulation of spouted beds, but also to set the operating conditions and to control spouting stability. Some authors have developed mathematical models for these variables that strongly depend on the characteristics of the particles, in addition to the configuration and geometry of the spouted bed [1,31, 32,35].

The inclined-blade stirrer showed no significant alteration of u_{sb} with increase of the rotation speed, although the lowest average value was obtained at 240 rpm (shown by the uppercase letters in Table 2). In contrast, the straight-blade stirrer showed the lowest u_{sb} value at 240 rpm, with higher rotation speeds not affecting this parameter [32]. These results indicate that the inclined-blade stirrer could be operated at a lower rotation speed, with a lower value of u_{sb}, enabling a reduction of energy consumption. Despite this behavior, the two stirrers showed similar results for u_{sb} at a rotation speed of 240 rpm, indicating that the effect of the type of stirrer was smaller at high rotation speeds.

Compared to the conventional spouted bed, the air velocity decreased at stirrer speeds above 60 rpm, with the exception of the screw-type stirrer. The latter showed a reduction of pressure peaks, compared to the CSB, even at low speeds, which could be attributed to a more homogeneous distribution of the air flow within the bed, irrespective of the rotation speed. This behavior is shown in Fig. 4 for the air velocity as a function of radial position.

As shown in Fig. 4(a), the straight-blade and screw-type stirrers presented flattened air velocity profiles, in agreement with literature data for these stirrers [32,33]. The profile for the inclined-blade stirrer is similar to that for the conventional spouted bed, but with lower velocity in the spout region. It is known that the conventional system presents low air velocity in the annular region, with a peak

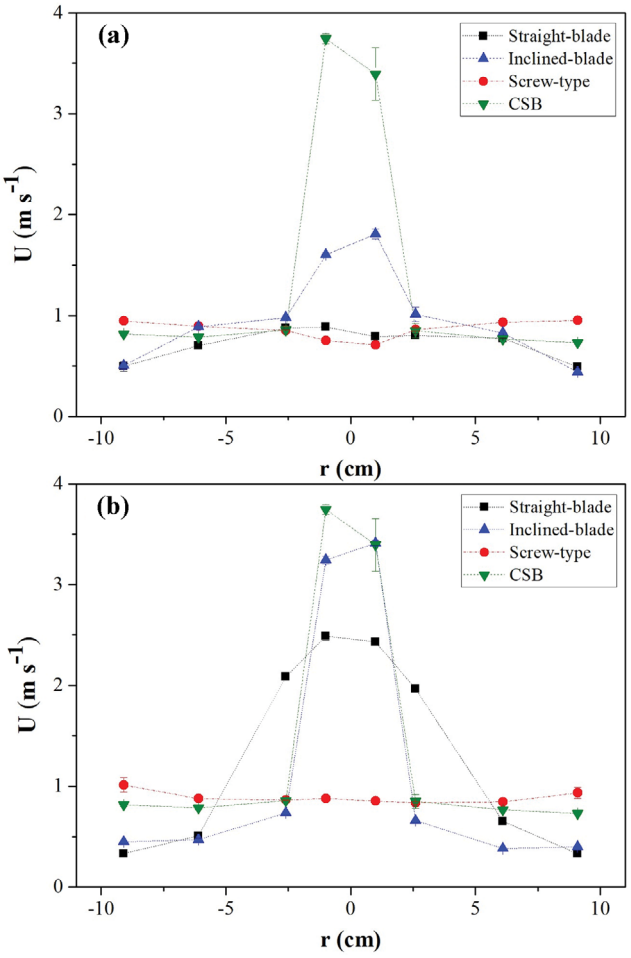

Fig. 4. Air velocity as a function of radius for the conventional and mechanically stirred spouted beds. Conditions: glass particles (d_p=2.2 mm and load of 3 kg), Q=0.88 $m^3 \cdot min^{-1}$ and z=0.05 m. (a) 60 rpm; (b) 120 rpm.

in the center of the bed, in the spout source region [1,43]. Similar regions are observed in the MMSSB, where the centripetal force caused by rotation of the stirrer throws the particles towards the equipment wall, forming an annular region with a higher concentration of solids. Consequently, a region of low solids concentration occurs in the center of the bed, forming a preferential channel, resulting in a functional alteration in the spout region, known as a "mechanical jet" [32,33,36]. In this region, the rotation speed and the type of stirrer affect the velocity profile, as shown in Fig. 4(b) for the 120 rpm rotation speed. Increase of the rotation speed acts to increase the size of the channel formed in the center of the bed, further facilitating passage of the air flow, as observed previously for straight-blade stirrers [32].

For the inclined-blade stirrer, the air velocity profile in the central region of the bed was similar to that for the conventional equipment, while there was a slight decrease in the annular region (Fig. 4(b)). This could be attributed to slow movement of particles near the wall, where there was no direct contact with the stirrer, so the air flow was restricted. In the case of the straight-blade stirrer, the air velocity in the center of the bed was lower, in comparison to

the inclined-blade stirrer and conventional systems. However, this profile changed in the annular region, due to widening of the channel produced by the stirrer in the center of the bed, as observed previously by Barros et al. [32].

Despite the higher rotation speeds of the screw-type stirrer, it did not present a different air velocity profile, although the velocity was slightly higher near the wall compared to the other stirrers, (Figs. 4(a) and 4(b)). In other work using a screw-type stirrer, the gas velocity profile was found to be affected by the rotation speed [35].

2. Relative Reduction of Air Flow - RR (%)

The results discussed above clearly evidence differences between the spouted beds with and without mechanical stirring, for both the fluid dynamic curve and the air velocity profile. In industrial applications, it is important that the inclusion of a stirrer should enable reduction of the air flow. This was evaluated using the dimensionless relative reduction (RR) parameter, calculated according to Eq. (1). Fig. 5 shows the results for RR as a function of rotation speed for the different stirrers.

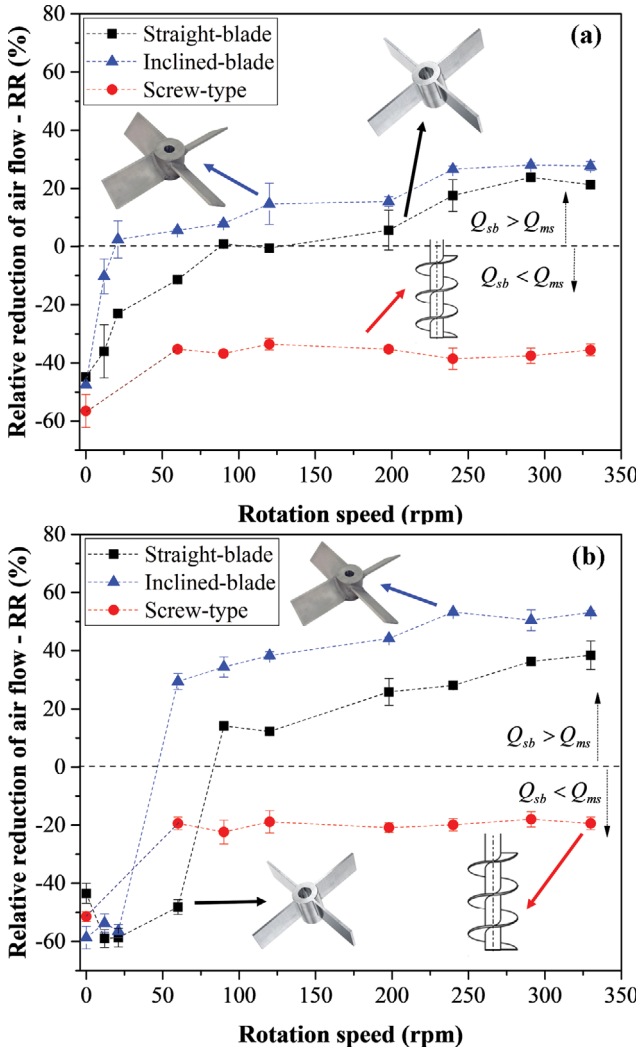

Fig. 5. Relative reduction (RR) of the air flow, as a function of stirrer rotation speed, for different stirrers, in comparison to the conventional equipment, using (a) 2 kg (assay E1) and (b) 4 kg (assay E3) of glass particles (d_p=2.2 mm).

Increase of the rotation speed led to higher RR, due to the greater movement of particles in the bed. At a rotation speed of 21 rpm, the inclined-blade stirrer showed zero relative reduction (Fig. 5(a)), with the air flows being the same for the MMSSB and the CSB (Q_{sb}=Q_{ms}), as indicated by the dotted line parallel to the rotation speed axis. In comparison with this stirrer, the straight-blade stirrer only reached the same RR at 90 and 120 rpm, while the screw-type stirrer presented lower values (−35%). These results indicate that the inclined-blade stirrer provides the best performance in terms of moving the particles in the bed.

Increase of the rotation speed had two main results. At around 240 rpm, there was no significant difference between RR for the straight-blade and inclined-blade stirrers. However, for the 4 kg load (Fig. 5(b)), the inclined-blade stirrer showed better performance, even at a rotation speed of 330 rpm. The maximum RR values were 28% and 53% for the 2 and 4 kg loads, respectively. The second observation was that constant RR could be obtained near 240 rpm, consequently decreasing the influence of the rotation speed (Figs. 5(a) and 5(b)). This could have been due to the size of the preferential channel formed in the center of the bed, which is a characteristic of blade-type stirrers.

Poorer RR results were obtained for the screw-type stirrer compared to the other systems, with no influence of the rotation speed. This result could be explained by the method used to determine the air flow required to agitate the bed (Q_{sb_3}), as indicated previously in Fig. 3. Although this method was based on fluid dynamics and information available in the literature, it is likely that it would be possible to use an air flow equal to that for the CSB, or even lower. Previous work showed that under the same operational drying conditions, there was no difference between the CSB and the MMSB in terms of kinetic parameters [39]. However, in the case of the specific energy consumption, the MMSB presented a reduction of 10%, despite problems such as particle agglomeration and the formation of dead zones [38,39]. These problems, which occurred close to the equipment wall, were due to the fact that the stirrer diameter was significantly smaller than that of the bed cylinder. This difficulty could be avoided using stirrers with sufficiently large diameter to "scrape" the equipment wall, increasing the region of direct movement of the particles, as in the case of the straight-blade and inclined-blade stirrers used in this study.

Despite the poor results for the screw-type agitator (Fig. 5), different behavior was expected for other groups of particles. Table 3 presents the data for the fluid dynamic parameters and RR for assays E2, E5, E8, E11, and E14, performed using the same particle mass and stirrer rotation speed.

For the screw-type stirrer, assay E2 (Glass-2.2 mm) showed a negative RR value of −18%, while assays E5 (Glass-4.4 mm) and E8 (Alumina-3.7 mm) showed positive values of around 20%. In the other assays, the values were close to zero. The results indicated that better performance of the screw-type stirrer was obtained with particles of glass (4.4 mm) and alumina. Nonetheless, for polyethylene particles (assays E11 and E14), it was still advantageous to use the equipment with mechanical agitation, in order to avoid instability in the bed and reduce pressure peaks [31,32,34].

For the inclined-blade stirrer, the lowest RR was observed with glass particles (E2), while the highest RR was with polyethylene

Table 3. Fluid dynamic parameters for the different stirrers, obtained using 3 kg of particles and a rotation speed of 240 rpm

Assay	Stirrers	u_{sb} (m s^{-1})	ΔP_s (Pa)	ΔP_{max} (Pa)	RR (%)
E2	CSB	21.8±0.5^{b}	1,140.0±10.0^{cb}	3,200.0±60.0a	---
	Straight-blade	14.8±0.3^{c}	1,090.0±60.0^{c}	1,400.0±200.0^{b}	32.0±1.0^{b}
	Inclined-blade	13.0±1.0^{c}	900.0±7.0^{a}	1,260.0±40.0^{b}	40.0±5.0^{b}
	Screw-type	26.0±1.0^{a}	1,220.0±60.0^{b}	1,220.0±60.0^{b}	−18.0±6.0^{a}
E5	CSB	42.0±1.0^{a*}	1,150.0±10.0^{ab}	3,150.0±20.0^{a}	---
	Straight-blade	23.0±1.0^{c}	1,190.0±20.0^{a}	1,280.0±30.0^{b}	46.0±3.0^{b}
	Inclined-blade	19.0±1.0^{c}	1,010.0±30.0^{c}	1,160.0±20.0^{c}	54.0±3.0^{b}
	Screw-type	33.0±4.0^{b}	1,090.0±50.0^{cb}	1,090.0±50.0^{c}	22.0±8.0^{a}
E8	CSB	37.5±0.1^{a}	940.0±8.0^{c}	2,480.0±10.0^{a}	---
	Straight-blade	21.0±4.0^{bc}	1,080.0±60.0^{a}	1,110.0±40.0^{b}	44.0±8.0^{ab}
	Inclined-blade	16.0±1.0^{c}	680.0±20.0^{b}	800.0±30.0^{d}	58.0±2.0^{a}
	Screw-type	27.0±4.0^{b}	910.0±40.0^{c}	910.0±40.0^{c}	27.0±8.0^{b}
E11	CSB	31.8±0.1^{c}	680.0±7.0^{a}	2,170.0±40.0^{a}	---
	Straight-blade	20.0±2.0^{a}	950.0±40.0^{c}	2,600.0±60.0^{b}	37.0±6.0^{b}
	Inclined-blade	11.8±0.3^{b}	520.0±20.0^{b}	7,40.0±30.0^{d}	62.9±0.7^{a}
	Screw-type	33.0±0.4^{c}	900.0±20.0^{c}	900.0±20.0^{c}	−4.0±1.0^{c}
E14	CSB	33.0±1.0^{c}	540.0±10^{c}	2,100.0±200^{c}	---
	Straight-blade	29.0±2.0^{a}	900.0±60.0^{b}	2,600.0±300^{c}	14.0±5.0^{b}
	Inclined-blade	11.4±0.2^{b}	490.0±3.0^{c}	660.0±20.0^{b}	65.8±0.5^{a}
	Screw-type	32.9±0.9^{c}	1,400.0±200^{a}	1,400.0±200^{a}	1.0±2.0^{c}

*Means followed by a different letter in a given column for each run (E2, E5, E8, E11, and E14) are significantly different at $p<0.05$ (Tukey's test).

particles (E14), obtaining values of around 40 and 66%, respectively. These results could be explained by the properties of the particles, as well as the greater static bed height for the polyethylene particles. When it is more difficult to move the particles and maintain a stable spout, the minimum spouting velocity (u_{mj}) is higher, so RR is also higher. This reveals an advantage of the MMSSB, since the movement of the particles is predominantly generated by the stirrer, requiring a lower air velocity and avoiding the "spout collapse" that can occur in conventional equipment. These results were corroborated by the fact that the u_{sb} values were always lower than u_{mj}, for all conditions using the inclined-blade and straight-blade stirrers.

The inclined-blade and straight-blade stirrers showed no significant differences in terms of RR and u_{sb} (Table 3), with the exception of assays E11 (ϕ=0.93) and E14 (ϕ=0.37) which could be attributed to instability in the equipment caused by greater static bed heights, resulting in bubbling or piston effects in the bed [32], leading to variation of the pressure drop. Consequently, the CSB presented a lower maximum pressure drop in the E14 assays, compared to the straight-blade system.

The poorest results were found for the straight-blade stirrer, because movement of the particles occurred mainly in the conical part of the bed, where there was direct contact with the stirrer. In the cylindrical part, the movement occurred indirectly by momentum transfer in the bed. For the inclined-blade stirrer, this phenomenon was minimized due to the angle of the blades, which assisted particle movement, favoring the formation of a channel in the center of the bed and facilitating the air flow.

Given the problems caused by a high bed height, the MMSSB design was altered, increasing the number of stirrer blades in order to reduce the air flow and improve the stability of the bed. The addition of another two blades (totaling five blades) provided agitation in the cylindrical part, rather than only in the conical base (obtained using three blades). This modification increased the height of the bed directly impacted by the stirrer blades. These assays were performed with the straight-blade stirrer, using particles of alumina (assays E7 and E8) and polyethylene (assays E10 and E11) (Fig. 6).

A significant difference in the RR values was only observed for

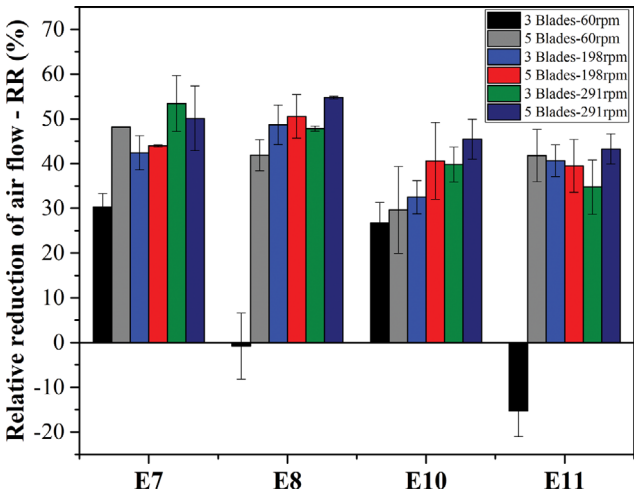

Fig. 6. Relative reduction of the air flow, as a function of rotation speed, for the straight-blade stirrer configurations with different numbers of blades (assays E7, E8, E10, and E11).

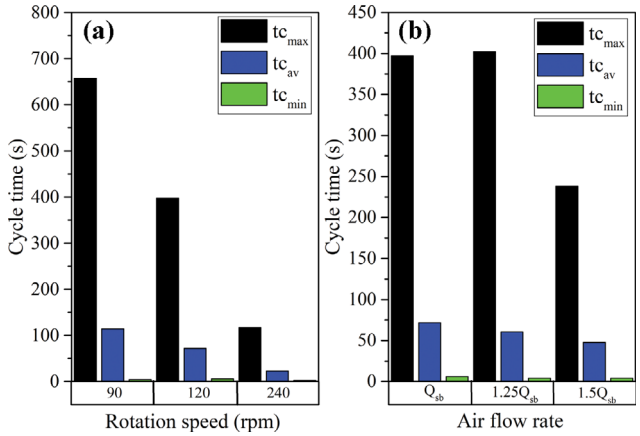

Fig. 7. Particle cycle time for straight-blade stirrer. (a) Q_{sb} for each rotation speed; (b) Rotation speed of 120 rpm.

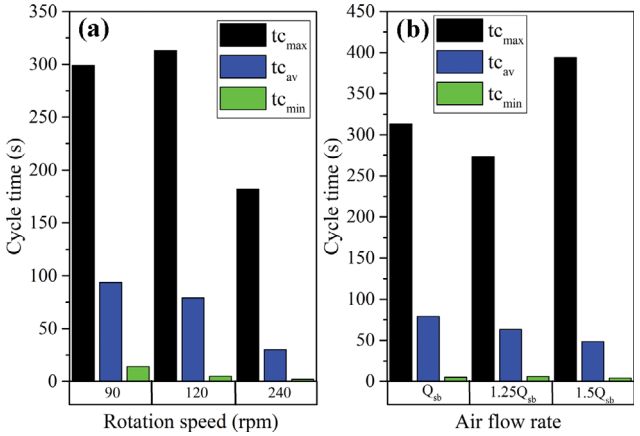

Fig. 8. Particle cycle time for inclined-blade stirrer. (a) Q_{sb} for each rotation speed; (b) Rotation speed of 120 rpm.

a rotation speed of 60 rpm, suggesting that the effect of the number of stirrer blades was not significant at higher rotation speeds (198 and 291 rpm). At 60 rpm, increase of the number of blades from three to five had a positive effect, with differences of RR of approximately 18, 43, 3, and 57% for assays E7 (Alumina-2 kg), E8 (3 kg), E10 (Polyethylene-2 kg), and E11 (3 kg), respectively. This showed that increasing the number of blades enabled the use of lower air flow rates at lower rotation speed, consequently reducing the energy cost. In addition, internal observation of the bed showed improvement in its stability, with bubbling bed formation being avoided when a stirrer with five blades was used. For the pressure drop in the bed, improved values of ΔP_{max} were obtained in the assays at 60 rpm. However, ΔP_{sb} increased when five blades were used, because the additional stirrer blades caused greater resistance to the air flow.

3. Average Cycle Time of Particles

The average cycle time was evaluated for the different configurations of the mechanical stirrers. The results of the maximum (tc_{max}), average (tc_{av}) and minimum (tc_{min}) cycle time are shown in Figs. 7, 8 and 9 for straight-blade, inclined-blade and screw-type.

It is shown in Fig. 7(a) that the rotation speed decreases the cycle time of the particles, although the airflow for 240 rpm is lower than for 90 rpm as it is based on the Q_{sb}. This shows that the cycle time of the particles depends more on the rotation speed than on the air flow. Thus, the average cycle time decreases by approximately 37% (90 to 120 rpm) and 68% (120 to 240 rpm). The maximum and minimum cycle time also decreases with increasing rotational speed. When analyzing the effect of air flow alone (Fig. 7(b)), there was a reduction of 16% between 1.00 Q_{sb} and 1.25 Q_{sb} and of 21% between 1.25 Q_{sb} and 1.50 Q_{sb}. Thus, these results show that there appears to be a combined effect of these two variables, at different levels.

In Fig. 8, the inclined-blade stirrer decreased the average cycle time by about 16% (90 to 120 rpm) and by 64% (120 to 240 rpm), the latter being higher than the process with straight-blade. The reduction was of 20% (1.00 Q_{sb} to 1.25 Q_{sb}) and of 24% (1.25 Q_{sb} to 1.50 Q_{sb}) for air flow, which were slightly higher than those of the straight-blade agitator. For the screw-type stirrer shown in Fig.

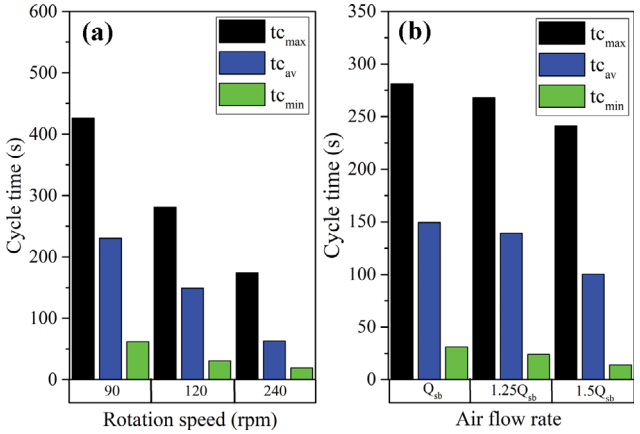

Fig. 9. Particle cycle time for screw-type stirrer. (a) Q_{sb} for each rotation speed; (b) Rotation speed of 120 rpm.

9, the maximum, average, and minimum cycle times decreased almost linearly with increasing rotation. The reduction was of approximately 35% (90 to 120 rpm) and 58% (120 to 240 rpm). Cycle time values as a function of rotational speed are in agreement with the literature [33-36]. Reyes et al. [23] showed that there was a decrease in the average residence time value with mechanical stirring in the particle bed.

As mentioned, the effect of each stirrer on the spouted bed depends on Q_{sb}, rotational velocity and fluid dynamic behavior. Therefore, it is difficult to compare the different agitators, since the experiments shown in Figs. 7-9 were done for different operating conditions. Thus, experiments were carried out with different agitators for the same rotation speed of 120 rpm and an air flow rate of 1.18 (Fig. 10(a)) and 1.41 $m^3 \cdot min^{-1}$ (Fig. 10(b)).

In the analysis of the different stirrers, it is observed that the stirrers blades have excelled compared to the helical screw of independent airflow employed. Compared to the screw, the inclined-blade stirrer showed a reduction of 53, 63 and 77% (Fig. 7(a)) for tc_{max}, tc_{av} and tc_{min}, respectively. For Fig. 7(b) the values were 32, 62 and 85%. In addition to these results, it is observed that an increase of 84% in the air flow (1.18 to 1.41 $m^3 \cdot min^{-1}$) caused a reduction in

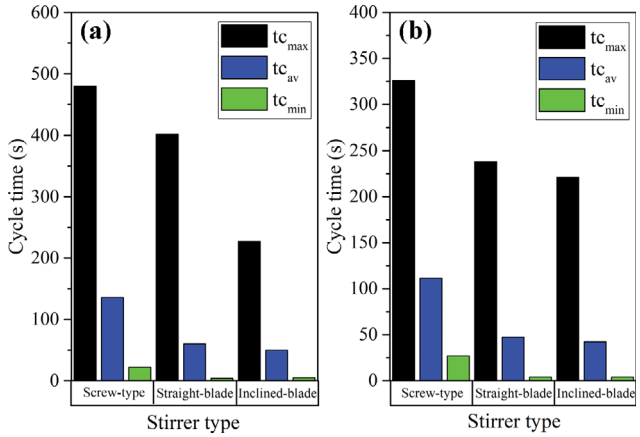

Fig. 10. Particle cycle time for different particle stirrers rotating at 120 rpm. (a) Air flow of 1.18 $m^3 \cdot min^{-1}$; (b) Air flow of 1.41 $m^3 \cdot min^{-1}$.

the average cycle time close to 82, 80 and 85% for the screw-type agitator, straight-blades and inclined-blades, respectively. This result suggests that there is a relationship between the increase in air flow and the reduction in the cycle time of the particles inside the bed. Such results are consistent with the literature since the increase in air flow provides a better mixing in the bed [44], which reduces the cycle time of the particles. In addition to air flow, other process parameters can affect the circulation time of particles inside the bed. Studies with internal devices such as draft tubes and fountain confiners have already indicated that the cycle time depends on the configuration used in the process [29]. Another study with Estiati et al. [45] pointed out that the increase in the angle, the height of the static bed, and the width of the sides of the draft tube lead to an increase in the average cycle times. In addition to geometric factors, Estiati et al. [45] reported that when operating conditions and cycle times are of the same order, drying time does

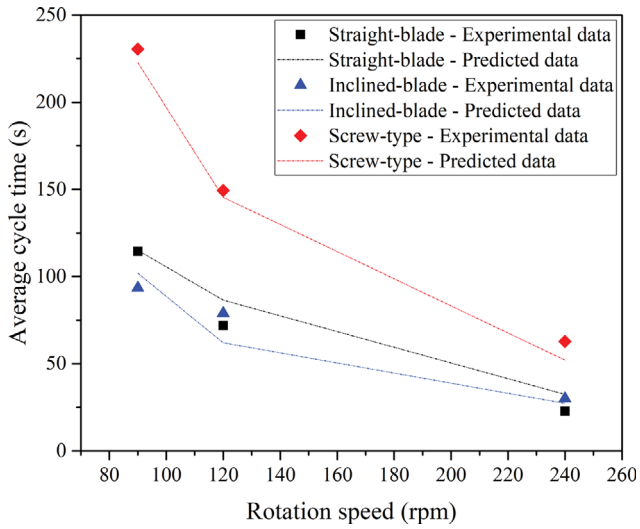

Fig. 11. Average cycle time of particles as a function of rotational speed for different stirrers based on Q_{sb}. Experimental data (points); Simulated data (lines).

not change significantly when scaling up.

In view of the results previously shown and the dependence of the process conditions on the cycle time, an empirical model was developed based on the speed of rotation and air flow, in addition to the characteristics of the particles and the stirrer. A general model was derived with a numerical value for each stirrer (St), 2, 4 and 6 for the screw-type, straight-blade and inclined-blade stirrers, respectively. The remaining variables of the model were given in the International Measurement System. The adjusted model is given by Eq. (2), with quadratic regression coefficient (R^2) of 0.927. Experimental and simulated data are shown in Fig. 11.

$$tc_{av}=1.265\ \Omega^{-1.482}Q^{-0.808}St^{-0.994}\frac{\rho_p H^{0.655}}{Md_p} \quad (2)$$

CONCLUSIONS

The use of stirrers in the particle bed led to improvement in the operational conditions of the equipment, with greater stability of the bed, reduction of the pressure drop, and lower air flow. The main conclusions of this work are the following:

- For straight-blade and inclined-blade agitators, the higher the rotation speed, the smaller the air flow required.
- The effect of blade inclination on fluid dynamics was smaller for 240 rpm;
- For the inclined-blade stirrer there was a relative reduction between 40-66% while the straight-blade was between 14-46% at 240 rpm.
- For the screw type agitator, there was a maximum relative reduction of 27%, depending on the characteristics of the particle and the load, although negative values were found in some of the experiments.
- For the screw type agitator, fluid dynamic parameters were not a function of the rotation speed.
- The decrease in airflow and pressure drop was greater for the inclined-blade stirrer.
- When compared to the conventional spouted bed, the setup with mechanical stirring system reduced the nominal and maximum pressure drop.
- For low rotational speeds, stirrers are not recommended because in this case the conventional spouted bed is more suitable.
- Increasing the number of stirrer blades can lead to a greater relative reduction in airflow, except at rotational speeds above 60 rpm.
- For the operational conditions of this work, the greater the number of blades, the better the stability of the spout, preventing against undesirable phenomena such as bubbling bed.
- The increase in airflow and especially in rotational speed led to a decrease in the average cycle time.
- The use of different groups of particles affected the operational parameters.

The addition of a stirrer in the bed provided significant operational advantages, offering the potential to increase the scale of industrial applications. Problems such as high pressure drop, bed instability, particle agglomeration, and accumulation of product in the bed can be minimized, while the lower air flow required to operate the

equipment can reduce operating costs. The findings presented here should encourage further studies of stirred particle beds, especially when these systems are used for particle coating, the drying of solids and pastes, and other applications requiring better control of particle movement.

ACKNOWLEDGEMENT

The authors appreciate the financial support provided by Coordination for the Improvement of Higher Education Personnel (CAPES, grant #88887.335028/2019-00).

NOMENCLATURE

CSB : conical spouted bed [-]
d_p : diameter of the particles [m]
FCC : face-centered central composite design [-]
H : static bed height [m]
M : bed mass [kg]
MMSB : modified mechanical spouted bed [-]
MMSSB : modified mechanical stirring spouted bed [-]
MSB : mechanical spouted bed [-]
MSSB : mechanically stirred spouted bed [-]
Q : air flow [$m^3 \cdot min^{-1}$]
Q_{sb} : air flow to stir the bed [$m^3 \cdot min^{-1}$]
Q_{ms} : minimum spout flow rate [$m^3 \cdot min^{-1}$]
RR : relative reduction of the air flow [%]
St : type of stirrer (2-screw; 4-straight-blade; 6-incline-blade)
tc_{av} : average cycle time [s]
tc_{max} : maximum cycle time [s]
tc_{min} : minimum cycle time [s]
u_{sb} : speed to stir the bed [$m \cdot s^{-1}$]
u_{ms} : speed minimum spouting [$m \cdot s^{-1}$]
ρ_p : particle density [$kg \cdot m^{-3}$]
ε : porosity of the bed [-]
ϕ : sphericity of the particles [-]
Ω : rotation speed [rpm]
ΔP_B : pressure drop in the bed [Pa]
ΔP_{max} : maximum pressure drop [Pa]
ΔP_s : stable spout pressure drop [Pa]
ΔP_{sb} : pressure drop of the stirred bed [Pa]

REFERENCES

1. K. B. Mathur and P. E. Gishler, *Spouted bed*, New York (1974).
2. J. T. Freire, M. C. Ferreira, F. B. Freire and B. S. Nascimento, *Dry. Technol.*, **30**, 330 (2012).
3. M. L. Passos, G. Massarani, J. T. Freire and A. S. Mujumdar, *Dry. Technol.*, **15**, 605 (1997).
4. A. P. T. Rocha, H. M. Lisboa, O. L. S. Alsina and O. S. Silva, *Powder Technol.*, **336**, 85 (2018).
5. M. Liu, Z. Chen, M. Chen, Y. Shao, B. Liu and Y. Tang, *Nucl. Eng. Des.*, **357**, 110413 (2020).
6. M. F. H. Wolff, V. Salikov, S. Antonyuk, S. Heinrich and G. A. Schneider, *Compos. Sci. Technol.*, **90**, 154 (2014).
7. L. Massaro Sousa and M. C. Ferreira, *Chem. Eng. Res. Des.*, **160**, 31 (2020).
8. S. Yang, R. Dong, Y. Du, S. Wang and H. Wang, *Energy*, **214**, 118839 (2021).
9. R. Martins, P. H. Britto-Costa and L. A. M. Ruotolo, *Environ. Technol.*, **33**, 1123 (2012).
10. J. Bilbao, M. Olazar, A. Romero and J. M. Arandes, *Ind. Eng. Chem. Res.*, **26**, 1297 (1987).
11. K. Azizi, M. Keshavarz Moraveji, A. Arregi, M. Amutio, G. Lopez and M. Olazar, *Bioresour. Technol.*, **311**, 123561 (2020).
12. K. M. Barcelos, P. S. Almeida, M. S. Araujo, T. P. Xavier, K. G. Santos, M. S. Bacelos and T. S. Lira, *Biomass Bioenergy*, **138**, 105592 (2020).
13. F. G. M. de Medeiros, I. P. Machado, T. N. P. Dantas, S. C. M. Dantas, O. L. S. de Alsina and M. F. D. de Medeiros, Transp. Process. Sep. Technol., in Spouted Bed Drying of Fruit Pulps: A Case Study on Drying of Graviola (Annona muricata), B. de L. A. Delgado J. (Ed.), Springer (2021).
14. J. P. A. A. Barros, M. C. Ferreira, J. T. Freire and M. C. Ferreira, *Dry. Technol.*, **38**, 1709 (2019).
15. R. C. Brito, M. B. Zacharias, V. A. Forti and J. T. Freire, *Dry. Technol.*, **39**, 820 (2020).
16. J. N. M. Batista, D. A. Santos and R. Béttega, *Particuology*, **54**, 91 (2021).
17. C. R. F. Souza and W. P. Oliveira, *Brazilian J. Chem. Eng.*, **22**, 239 (2005).
18. N. Barret and A. Fane, Drying Liquid Materials in a Spouted Bed (1990).
19. T. Szentmarjay, E. Pallai, Tóth J, Mechanical spouting, in: S. and spouted-fluid beds: F. and applications N. Epstein, & J. R. Grace (Ed.), In. N. Epstein, J. R. Grace, Spouted Spouted-Fluid Beds Fundam. Appl., Cambridge University Press, New York, 297 (2011).
20. M. L. Passos, A. S. Mujumdar, G. Vijaya and V. G. S. Raghavan, *Dry. Technol.*, **7**, 663 (1989).
21. I. Puspasari, M. Zainal, M. Talib, W. Ramli, W. Daud, S.0 M. Tasirin, I. Puspasari, M. Zainal, M. Talib, W. Ramli and W. Daud, *Dry. Technol.*, **30**, 619 (2012).
22. R. G. Bait, S. B. Pawar, A. N. Banerjee, A. S. Mujumdar and B. N. Thorat, *Dry. Technol.*, **29**, 808 (2011).
23. A. Reyes, G. Díaz and F. H. Marquardt, *Dry. Technol.*, **19**, 2235 (2001).
24. T. Reed, III and M. Fenske, *Ind. Eng. Chem.*, **47**, 275 (1955).
25. M. Olazar, M. J. San José, A. T. Aguayo, J. M. Arandes and J. Bilbao, *Ind. Eng. Chem. Res.*, **31**, 1784 (1992).
26. M. Olazar, M. J. San José, R. Aguado, B. Gaisán and J. Bilbao, *Ind. Eng. Chem. Res.*, **38**, 4120 (1999).
27. I. Estiati, M. Tellabide, J. F. Saldarriaga, H. Altzibar and M. Olazar, *Powder Technol.*, **356**, 193 (2019).
28. M. Karimi, B. Vaferi, S. H. Hosseini, M. Olazar and S. Rashidi, *Particuology*, **55**, 179 (2021).
29. J. F. Saldarriaga, I. Estiati, A. Atxutegi, R. Aguado, J. Bilbao and M. Olazar, *Ind. Eng. Chem. Res.*, **58**, 1932 (2019).
30. S. H. Hosseini, M. J. Rezaei, M. Bag-Mohammadi, H. Altzibar and M. Olazar, *Chem. Eng. Res. Des.*, **138**, 331 (2018).
31. A. Reyes and I. Vidal, *Dry. Technol.*, **18**, 341 (2000).
32. J. P. A. de A. Barros, R. C. Brito, F. B. Freire and J. T. Freire, *Ind. Eng. Chem. Res.*, **59**, 16396 (2020).
33. T. Szentmarjay and E. Pallai, *Dry. Technol.*, **7**, 523 (1989).

34. J. Németh, E. Pallai and E. Aradi, *Can. J. Chem. Eng.*, **61**, 419 (1983).
35. T. Szentmarjay, A. Szalay and I. Pallai, *Hungarian J. Ind. Chem. Veszprém.*, **20**, 219 (1992).
36. J. Németh, E. Pallai, M. Péter and R. Toros, *Can. J. Chem. Eng.*, **61**, 406 (1983).
37. T. Kudra, E. Pallai, Z. Bartczaki and M. Peter, *Dry. Technol.*, **7**, 583 (2007).
38. R. C. Sousa, M. C. Ferreira, H. Altzibar, F. B. Freire and J. T. Freire, *Particuology*, **42**, 176 (2019).
39. R. C. Brito, R. C. Sousa, R. Béttega, F. B. Freire and J. T. Freire, *Chem. Eng. Process. Process Intensif.*, **130**, 1 (2018).
40. G. N. A. Vieira, F. B. Freire and J. T. Freire, *Dry. Technol.*, **33**, 1920 (2015).
41. D. Geldart, *Powder Technol.*, **7**, 285 (1973).
42. K. B. Mathur and N. Epstein, *Spouted beds*, Academic Press, New York (1974).
43. T. Mamuro and H. Hattori, *J. Chem. Eng. Japan.*, **1**, 1 (1968).
44. H. Altzibar, G. Lopez, J. Bilbao and M. Olazar, *Can. J. Chem. Eng.*, **91**, 1865 (2013).
45. I. Estiati, H. Altzibar, M. Tellabide and M. Olazar, *Powder Technol.*, **316**, 87 (2017).